HHS Public Access

Author manuscript

Mater Sci Eng C Mater Biol Appl. Author manuscript; available in PMC 2017 March 01.

Published in final edited form as:

Mater Sci Eng C Mater Biol Appl. 2016 March 1; 60: 324–332. doi:10.1016/j.msec.2015.11.039.

Preparation of resorbable carbonate-substituted hollow hydroxyapatite microspheres and their evaluation in osseous defects in vivo

Wei Xiao[1], **B. Sonny Bal**[2], and **Mohamed N. Rahaman**[1,*]

[1]Department of Materials Science and Engineering, Missouri University of Science and Technology, Rolla, Missouri 65409

[2]Department of Orthopaedic Surgery, University of Missouri, Columbia, Missouri 65212

Abstract

Hollow hydroxyapatite (HA) microspheres, with a high-surface-area mesoporous shell, can provide a unique bioactive and osteoconductive carrier for proteins to stimulate bone regeneration. However, synthetic HA has a slow resorption rate and a limited ability to remodel into bone. In the present study, hollow HA microspheres with controllable amounts of carbonate substitution (0–12 wt. %) were created using a novel glass conversion route and evaluated in vitro and in vivo. Hollow HA microspheres with ~12 wt. % of carbonate (designated CHA12) showed a higher surface area (236 m^2g^{-1}) than conventional hollow HA microspheres (179 m^2g^{-1}) and a faster degradation rate in a potassium acetate buffer solution. When implanted for 12 weeks in rat calvarial defects, the CHA12 and HA microspheres showed a limited capacity to regenerate bone but the CHA12 microspheres resorbed faster than the HA microspheres. Loading the microspheres with bone morphogenetic protein-2 (BMP2) (1 μg per defect) stimulated bone regeneration and accelerated resorption of the CHA12 microspheres. At 12 weeks, the amount of new bone in the defects implanted with the CHA12 microspheres (73 ± 8 %) was significantly higher than the HA microspheres (59 ± 2%) while the amount of residual CHA12 microspheres (7 ± 2% of the total defect area) was significantly lower than the HA microspheres (21 ± 3%). The combination of these carbonate-substituted HA microspheres with clinically safe doses of BMP2 could provide promising implants for healing non-loaded bone defects.

Keywords

Hollow hydroxyapatite microspheres; resorbable hydroxyapatite; bone regeneration; bone morphogenetic protein-2; rat calvarial defect model

* Corresponding author. Tel.: +1 573 341 4406; fax: +1 573 341 6934, rahaman@mst.edu (M.N. Rahaman).

1. Introduction

The healing of large bone defects resulting from trauma, resection of tumors or congenital diseases represents a common and significant problem in craniofacial and orthopedic surgery. Clinically those defects are reconstructed using autologous bone grafts, allografts and biocompatible synthetic materials [1–3]. Autologous bone grafts are the gold standard for treatment while bone allografts are the most commonly used bone grafts. However, they suffer from limitations such as limited supply, donor site morbidity (autografts), high cost, uncertain healing and risk of infection (allografts) [4]. Because of these limitations, the need for synthetic biomaterials continues to grow.

A variety of synthetic bone graft substitutes have been developed over the last several decades [1, 2]. They include calcium phosphate bioceramics such as hydroxyapatite (HA), beta-tricalcium phosphate (β-TCP), biphasic calcium phosphate (BCP), calcium phosphate cements, bioactive glass and biodegradable polymers. However, synthetic bone graft materials generally lack the osteoinductivity and osteogenicity of autogenous bone grafts, functioning mainly as osteoconductive implants [1, 5–7]. The use of synthetic biomaterials by themselves commonly fails to produce clinically significant bone formation in a clinically relevant time [7, 8]. In practice, synthetic biomaterials are often combined with autologous bone, osteogenic growth factors or cells in order to achieve reliable reconstruction of bone [7, 9-11].

Calcium phosphate bioceramics such as HA, β-TCP and BCP have been used in dentistry and medicine for bone repair and augmentation for over 30 years [12, 13]. They have a high affinity for binding and concentrating proteins which make them ideal carriers for growth factors such as bone morphogenetic protein-2 (BMP2) and bioactive peptides [14, 15]. Several studies have shown that when combined with BMP2, calcium phosphate bioceramics in the form of porous particles, granules or three-dimensional scaffolds enhanced osteogenesis in animal models when compared to the calcium phosphate bioceramics without BMP2 [16-21].

HA is often considered to be a prototype biomaterial for bone repair and augmentation because of its similarity to the mineral constituent of living bone [22]. However, synthetic HAs with a nearly stoichiometric composition often have a low resorption rate, resulting in the material remaining nearly bioinert in vivo over a long period [23, 24]. In comparison, biological HAs contain minor and trace elements and are therefore not pure HA. The most important minor substituents are CO_3, Mg and Sr. The ability of the implant to remodel into bone within a clinically relevant time is desirable for bone repair. The degradation of HA and other calcium phosphate bioceramics can occur by two processes: solution-mediated dissolution [14, 23], and cell-mediated degradation resulting from the activities of osteoclastic cells [25–27]. Ionic substitution by $(CO_3)^{2-}$, Mg^{2+} and Sr^{2+}, fine particle size, high surface area and high porosity have been shown to improve the solution-mediated degradation rate of HA [14, 27–30] whereas $(CO_3)^{2-}$ substitution and fine grain size have been found to be desirable for osteoclastic resorption [25, 26].

In the last few years, we have been developing a hollow HA microsphere technology to address the need for bone graft substitutes that could approach the combined osteoconductive, osteoinductive and osteointegrative properties of autologous bone grafts. The hollow HA microspheres, prepared by a novel glass conversion route near room temperature, have a high surface area (>100 m^2 g^{-1}) and a mesoporous shell wall (pore size = 10–20 nm) composed of nanocrystalline HA particles [31]. Our previous studies showed that hollow HA microspheres can function as a carrier for the controlled delivery of proteins and growth factors [32, 33]. When loaded with BMP2 (1 μg per defect), the hollow HA microspheres (106–150 μm) enhanced bone regeneration in rat calvarial defects (4.6 mm in diameter) when compared to similar microspheres without BMP2, resulting in bridging of the defects by new bone within 6 weeks [33]. However, little resorption of the HA microspheres was observed in the defects within the six-week implantation period.

The objective of this study was to create hollow HA microspheres with a faster degradation rate and test their performance in vitro and in vivo. The glass conversion process used in our previous studies was modified to create hollow HA microspheres with controllable amounts of $(CO_3)^{2-}$ substitution. Carbonate-substituted HA compositions were used because they have been shown to result in enhanced degradation or resorption rates. The dissolution of the microspheres in a potassium acetate buffer solution and their degradation by osteoclastic cells was studied in vitro. Microspheres with or without BMP2 were implanted in rat calvarial defects in vivo and their ability to resorb and to regenerate bone was evaluated at 12 weeks postimplantation using histomorphometric methods.

2. Materials and Methods

2.1 Preparation and characterization of hollow HA microspheres

Hollow HA microspheres with a nearly stoichiometric composition were prepared by reacting solid glass microspheres in an aqueous phosphate solution, as described in detail in our previous study [31]. Briefly, borate glass microspheres (150–250 μm) with the composition 15CaO, 11Li_2O, 74B_2O_3 (wt. %) were reacted for 7 days in 0.02 M K_2HPO_4 solution at 37 °C and starting pH = 9.0. A mass of 4 g glass microspheres was reacted in 800 ml of the phosphate solution in all of the conversion experiments. The converted microspheres were washed 3 times with deionized water, soaked in anhydrous ethanol to displace residual water, and dried for at least 12 h at room temperature then for at least 12 h at 90 °C. Carbonate-substituted HA (CHA) microspheres with varying carbonate content were prepared using the same method but the phosphate solution used in the conversion process contained different concentrations of carbonate ions by adding $KHCO_3$ to the solution (**Table I**).

Characterization of the converted microspheres (HA and CHA) was performed using the methods described previously [31]. Briefly, the microstructure of the surface and cross section of the microspheres was examined using scanning electron microscopy (SEM) (S4700; Hitachi, Tokyo, Japan). X-ray diffraction (XRD) (D/mas 2550 v; Rigaku; The Woodlands, TX, USA) was used to check for the presence of crystalline phases in the converted microspheres while Fourier transform infrared (FTIR) spectroscopy (NEXUS 670; Thermo Nicolet; Madison, WI, USA) was used to determine the chemical groups in the

composition. The specific surface area, average pore size and pore size distribution of the shell of the converted microspheres were measured using nitrogen adsorption (Autosorb-1; Quantachrome, Boynton Beach, FL, USA). In addition, the carbon content of the converted microspheres was determined at a commercial laboratory using a Carbon/Sulfur Analyzer (CS844; LECO Corp.; St. Joseph, MI, USA) designed to measure the carbon and sulfur content in metals and ceramics using a combustion method. Three samples from each group of microspheres were analyzed and the carbonate content was determined by assuming that all the measured carbon in the microspheres was present as carbonate (CO_3).

2.2 Degradation of hollow HA and CHA microspheres in vitro

The solubility of the converted microspheres was determined by measuring the concentration of Ca^{2+} ions released from the microspheres as a function of immersion time in an acidic buffer (0.1 M potassium acetate; pH = 5.0) at 37 °C [23, 34], using inductively-coupled plasma optical emission spectrometry (ICP-OES) (Optima 2000DV; Perkin Elmer, Waltham, MA). A fixed surface area to volume ratio (50 $m^2\ l^{-1}$) of HA microspheres to potassium acetate solution was used. Three samples from each group were analyzed at each time point. The solubility of granules composed of medical grade beta-tricalcium phosphate (β-TCP) (Himed; Old Bethage, NY) was used as a reference for comparison.

2.3 Osteoclastic resorption of hollow HA and CHA microspheres in vitro

Cell-mediated degradation of the converted microspheres was studied using induced osteoclast cultures [26, 35]. The human monocyte-like cell line TIB-71 (ATCC, USA) was cultured in Dulbecco's modified Eagle's medium (DMEM) supplemented with 10 vol. % fetal bovine serum (FBS) (Sigma-Aldrich, St. Louis, MO) and 1 vol. % penicillin/streptomycin (Invitrogen) at 37 °C in a humidified atmosphere of 5% CO_2. The microspheres were sterilized by soaking in anhydrous ethanol and exposure to ultraviolet light. Then TIB-71 cells were seeded at a concentration of 10^5 cells per ml and incubated at 37 °C in a humidified CO_2 atmosphere. At day 1, 50 ng/ml RANKL (Biolegend, San Diego, CA) was added to the culture media to induce the differentiation of the TIB-71 cells to osteoclasts. The media was replaced with fresh media containing 50 ng per ml RANKL every 2 days for the remainder of the experiment.

The microspheres were removed from the culture media at day 7 and rinsed with 0.1 M phosphate-buffered saline (PBS). Then the cells were fixed with 2% paraformaldehyde plus 2% glutaraldehyde in 0.1 M cacodylate buffer overnight at 4 °C. Each sample was rinsed with 0.1 M cacodylate buffer and fixed in 2% osmium tetroxide for 2 h at room temperature. The fixed samples were dehydrated in a graded ethanol series, soaked in hexamethyldisilazane (HMDS) and dried in air to allow the liquid to fully evaporate. The dried samples were sputter-coated with gold and observed in a scanning electron microscope (S-4700; Hitachi) at an accelerating voltage of 15 kV and a working distance of 13 mm.

2.4 Animals and surgery

Hollow HA and CHA microspheres, as-prepared or loaded with BMP2, were implanted in rat calvarial defects to evaluate their response in osseous defects. After being sterilized by soaking in anhydrous ethanol and exposure to ultraviolet light, the microspheres were loaded

with BMP2 using a procedure described in detail in our previous study [33]. Briefly, 10 mg of hollow microspheres were placed in a 1 ml centrifuge tube, and 10 μl of BMP2 solution, formed by dissolving 10 μg BMP2 (Shenandoah Biotechnology Inc., Warwick, PA) in 100 μl sterile citric acid (pH = 3.0), was pipetted onto the microspheres. A small vacuum was applied to the system to replace the air in the hollow microspheres with the BMP2 solution. The BMP2 solution was completely absorbed in the microspheres. The BMP2-loaded microspheres were dried overnight in a refrigerator at 4 °C until used in the animal experiments the following day.

All animal experimental procedures were approved by the Missouri University of Science and Technology Animal Care and Use Committee, in compliance with the NIH Guide for Care and Use of Laboratory Animals (1985). Sprague Dawley rats (3 months old; 350 ± 30 g) were housed in the animal care facility and acclimated to diet, water and housing under a 12h/12h light/dark cycle. The rats were anesthetized with an intramuscularly injected mixture of ketamine and xylazine (1.5 μl/kg). The surgical area was shaved, scrubbed with 70% ethanol and iodine, and then draped. With sterile instruments and an aseptic technique, a cranial skin incision was sharply made in an anterior to posterior direction along the midline. The subcutaneous tissue, musculature and periosteum were dissected and reflected to expose the calvarium. Bilateral full-thickness defects 4.6 mm in diameter were created in the central area of each parietal bone using a PBS-cooled trephine drill without disturbing the dura mater. The sites were constantly irrigated with sterile PBS to prevent overheating of the bone margins and to remove the bone debris. The bilateral defects were randomly implanted with 7 replicates per group but microspheres with and without BMP2 were not mixed in the same animal. Each defect was implanted with the same mass of microspheres (10 mg). The number of replicates per group (n = 7) was based on our previous studies [33]. The periosteum and skin were repositioned and closed using wound clips. The animals were given a dose of ketoprofen (3 mg per kg mass of the animal) intramuscularly and 0.2 ml penicillin subcutaneously post-surgery, and they were monitored daily for the condition of the surgical wound, food intake, activity and clinical signs of infection. After 12 weeks, the animals were sacrificed by CO_2 inhalation and the calvarial defects with surrounding bone and soft tissue were harvested for subsequent evaluation. This implantation was used because our previous study showed that for the same animal model, the amount of new bone in the defects implanted with the HA microspheres without BMP2 was limited [33].

2.5 Histologic processing

The harvested calvarial samples were fixed in 10% formaldehyde for 5 days, washed with deionized water and then cut in half. Half of each sample was for paraffin embedding while the other half was for poly(methyl methacrylate) (PMMA) embedding. The samples for paraffin embedding were decalcified in 14% ethylenediaminetetraacetic acid (EDTA) for 2 weeks, dehydrated in a graded series of ethanol and embedded in paraffin using routine histological techniques. Then the samples were sectioned to 5 μm using a microtome and stained with hematoxylin and eosin (H&E). The un-decalcified samples were dehydrated in a graded series of ethanol and embedded in PMMA. Sections were affixed to acrylic slides, ground down to 40 μm using a surface grinder (EXAKT 400CS, Norderstedt, Germany) and stained using the von Kossa method. Transmitted light images of the stained sections were

taken with an Olympus BX 50 microscope connected to a CCD camera (DP70, Olympus, Japan).

2.6 Histomorphometric analysis

Histomorphometric analysis was carried out using optical images of the stained sections and the ImageJ software (National Institutes of Health, USA). One section across the diameter of each defect was analyzed. The amount of new bone and residual HA (or CHA) microspheres in the defects were evaluated from the H&E stained sections. The entire defect area was determined as the area between the two defect margins, including the HA microspheres and the tissues. The newly formed bone and residual microspheres within the defect area were then outlined and measured. The area of new bone and residual HA microspheres was expressed as a percentage of the total defect area. The von Kossa-positive area in the defects implanted with microspheres was determined from the von Kossa stained sections, which yielded the combined amount of mineralized bone and hydroxyapatite as both bound the silver nitrate.

2.7 Statistical analysis

The data are presented as a mean ± standard deviation (SD). Analysis for differences between groups was performed using one-way analysis of variance (ANOVA) with Tukey's post hoc test. Differences were considered significant for $p < 0.05$.

3. Results

3.1 Characteristics of converted microspheres

The BET surface area, average pore size (diameter or width) and carbonate content of the three groups of converted microspheres used in the present study (external diameter = 150–250 μm) are summarized in **Table I**. The microspheres designated HA, corresponded to the microspheres used in our previous studies [31–33]. The carbonate content of those HA microspheres was not determined previously but the results of the present study showed that they contained 2.1 wt. % carbonate. The carbonate substitution presumably resulted from dissolved CO_2 in the aqueous phosphate solution used in converting the glass microspheres to hydroxyapatite microspheres. However, for consistency with our previous studies, we will continue to refer to those microspheres as HA microspheres. The microspheres formed by conversion in the aqueous phosphate solutions that contained 0.135 and 0.27 M $KHCO_3$, with a carbonate content of 8.6 and 12.4 wt. %, respectively, will be referred to as CHA9 and CHA12. The surface area of the CHA9 and CHA12 microspheres was higher than the HA microspheres, presumably because of a finer particle (or pore) size. The average pore size of the shell was 11, 8 and 7 nm, respectively, for the HA, CHA9 and CHA12 microspheres.

SEM images of the cross section of the microspheres confirmed that they were hollow (**Fig. 1**). The surface of the HA microspheres showed needle-like particles, similar to those for the HA microspheres prepared previously [31–33]. In comparison, the surface of the CHA9 and CHA 12 microspheres was composed of nearly spherical particles. The peaks in the XRD patterns of the HA, CHA9 and CHA12 microspheres corresponded to a reference

hydroxyapatite (JCPDS 72-1243) (**Fig. 2a**). However, the height of the major peak for the CHA 9 and CHA12 groups decreased by 30% and 40%, respectively, and the half-width increased by 10% and 15%, respectively, relative to the major peak for the HA group.

The most dominant resonances in the FTIR spectra (**Fig. 2b**) of the three groups of microspheres were the phosphate ν3 resonance, centered at ~1,040 cm^{-1}, and the phosphate ν4 resonance with peaks at ~605 and 560 cm^{-1} that are associated with crystalline HA [37, 38]. The peaks at ~1450–1490 cm^{-1} are associated with the C–O ν3 resonance while the peak at 875 cm^{-1} is associated with the CO_3^{2-} ν2 resonance [39]. The increase in peak area from HA to CHA12 indicated an increase in carbonate content, in accordance with the results of **Table I**. These resonances also indicated that a B-type substitution in which carbonate ions substitute for the phosphate ions in the hydroxyapatite lattice [40].

3.2 Solution mediated degradation in vitro

The solution-mediated degradation of hydroxyapatite is generally considered to be a congruent process, so the dissolution rate can be described by the rate of Ca^{2+} ion release. The cumulative amount of Ca^{2+} ions released from the HA, CHA9 and CHA12 microspheres into the potassium acetate buffer solution (at a constant surface area to volume ratio) is shown as a function of immersion time in **Fig. 3a.** The release profiles of the three groups of microspheres showed the same trend. The release was more rapid initially (up to ~10 h), slowed considerably thereafter and almost ceased after ~24 h. At any immersion time, the amount of Ca^{2+} ions released into the medium increased with the carbonate content of the microspheres. However, the amount of Ca^{2+} ions released from the CHA12 microspheres was still considerably lower than the β-TCP reference material. The amount of Ca^{2+} ions released into the medium at an immersion time of 1 h (**Fig. 3b**) showed a significant increase with increasing carbonate substitution but the amount of Ca^{2+} ions released from the CHA12 microspheres was significantly smaller than the β-TCP reference material.

3.3 Cell mediated degradation in vitro

After 7 days of incubation, giant cells with multiple nuclei were found on the surface of microspheres (**Fig. 4a1-3**). These osteoclast-like cells had an average size of ~50 μm. After the cells were rinsed off, pits became visible on the surface of the microspheres (**Fig. 4b1-3**), showing degradation of the microspheres by the osteoclastic cells. The surface of the CHA12 microspheres appeared to have deeper pits than the HA and CHA9 microspheres. However, because of curved surface of the microspheres and the size of the cells relative to the microsphere diameter, the amount of the pitted area, as a fraction of the surface area of the microspheres could not be readily quantitated.

3.4 Bone regeneration in rat calvarial defects in vivo

Optical images of the H&E stained sections of the rat calvarial defects implanted with the HA and CHA12 microspheres without BMP2 are shown in **Fig. 5**. For both implant groups, new bone formation was limited and it was confined mainly to the edge (periphery) of the defect. Although the same mass of HA and CHA12 microspheres was implanted in the defects, the amount of CHA12 microspheres remaining in the defects (28 ± 8% of the total

defect area) was smaller than the HA microspheres (34 ± 10%) but the difference was not significant (**Fig. 5a, b**). Several CHA12 microspheres were composed of open (or incomplete) microspheres (**Fig. 5a; arrows**) in which a large segment of the shell was missing. These open microspheres were filled with fibrous (soft) tissue. They were presumably formed as a result of resorption in vivo. The number of open microspheres normalized to the total number of microspheres was 27 ± 4% and 4 ± 4%, respectively, for the CHA12 and HA groups. Higher magnification images (**Fig. 5c, d**) of the boxed areas in **Fig. 5a, b** show a comparison of the open CHA12 microspheres and the closed HA microspheres. While it is possible that the CHA12 microspheres could have a lower strength than the HA microspheres, it appears unlikely that the higher percent of open CHA12 microspheres was due to a lower strength. The calvarial defect is a non-loaded site and implantation of the microspheres required little force. Furthermore, no broken pieces of CHA12 or HA microspheres were observed during preparation and implantation of the microspheres.

H&E and von Kossa stained sections of the defects implanted with BMP2-loaded CHA12 and HA microspheres for 12 weeks are shown in **Fig. 6**. Loading the microspheres with BMP2 significantly enhanced their capacity to heal the defects. New bone almost completely infiltrated the pore space between the microspheres and bridged the ends of the defect. The percent new bone in the defects implanted with the BMP2-loaded CHA12 microspheres (73 ± 9%) was significantly greater than the BMP2-loaded HA microspheres (59 ± 2%) (**Fig. 7**). The percent CHA12 microspheres remaining in the defects at 12 weeks (7 ± 2% of the total defect area) was significantly lower than the HA microspheres (21 ± 3%). The images of the H&E stained sections showed that some marrow-like tissue was present in the defect space not occupied by new bone and residual HA or CHA microspheres which is often a feature of bone regeneration stimulated by the use of BMP2 [41–43].

4. Discussion

Hollow HA microspheres, with a high-surface-area mesoporous shell, can provide a unique osteoconductive and bioactive carrier for the local delivery of therapeutics (such as proteins) in bone repair [32, 33]. However, HA with a nearly stoichiometric composition has a slow resorption rate and its ability to remodel into bone is limited. The results of the present study showed that partial substitution of the phosphate $(PO_4)^{3-}$ ions with carbonate $(CO_3)^{2-}$ ions in the HA enhanced the degradation or resorption rate of the microspheres. The enhanced resorption rate of the carbonate-substituted hydroxyapatite (CHA) microspheres did not enhance their capacity to regenerate bone in rat calvarial defects when compared to the HA microspheres. Loading the HA and CHA microspheres with BMP2 significantly improved bone regeneration. Defects implanted with the BMP2-loaded CHA microspheres showed significantly higher new bone formation and lower residual microsphere material at 12 weeks when compared to the BMP2-loaded HA microspheres. These CHA microspheres, when loaded with clinically safe doses of BMP2, are promising implants for regenerating bone in non-loaded defects, such as defects in the craniofacial region.

4.1 Properties of carbonate-substituted HA microspheres in vitro

The conversion of borate glass microspheres to hollow HA microspheres in an aqueous phosphate solution near room temperature has been described in detail previously [31]. As the glass degrades, the Ca^{2+} ions released from the glass react with the $(PO_4)^{3-}$ ions from the solution to form an amorphous calcium phosphate product on the glass surface which subsequently crystallizes to HA. In the present study, varying concentrations of $(CO_3)^{2-}$ ions were added to the phosphate solution with the objective of forming hollow microspheres composed of carbonate-substituted hydroxyapatite (CHA). The results showed that hollow CHA microspheres were formed and that the amount of carbonate substitution increased with higher amounts of $(CO_3)^{2-}$ ions in the starting phosphate solution.

The amount of carbonate in human bone mineral is ~8 wt. % [44]. In the present study, hollow HA microspheres, similar to the microspheres used in our previous studies (which contained 2.1 wt. % carbonate) and hollow CHA microspheres with 8.6 and 12.4 wt. % carbonate were prepared and evaluated. It is likely the higher amounts of carbonate could be incorporated into the hollow HA microspheres but that was not investigated. Substitution of Mg^{2+} and Sr^{2+} has also been shown to enhance the degradation rate of HA [27–30] and it is expected that substitution of those ions could also be achieved in the glass conversion route used in the present study.

The FTIR data indicated a B-type substitution in which $(CO_3)^{2-}$ ions substituted for the $(PO_4)^{3-}$ ions in the hydroxyapatite lattice [40] which is generally found in typical biological HAs and synthetic HAs formed by precipitation from solution [39]. XRD indicated that the carbonate substitution reduced the crystallinity of the HA. The major hydroxyapatite peak in the XRD pattern showed a decrease in height and an increase in half-width with increasing carbonate (**Fig. 2a**). SEM showed that the needle-like particle morphology on the surface of the hollow HA microspheres changed to a more rounded morphology on the surface of the CHA microspheres (**Fig. 1**), while the BET surface area of the CHA microspheres were higher than the HA microspheres. A reduction in crystallinity and particle size has been observed previously for B-site substituted HA [45, 46].

The solubility of the hollow HA microspheres, as measured by the release of Ca^{2+} ions in a potassium acetate buffer solution (pH = 5.0) at 37 °C increased with higher carbonate content (**Fig. 3a**), which is compatible with the results of previous studies [23, 30, 47]. As a constant surface area to volume ratio was used in the experiments, the increase in solubility was presumably due to a reduction in crystallinity of the hollow CHA microspheres. The amount of Ca^{2+} ions released from the CHA12 microspheres into the buffer solution at 1 h was more than twice the value from the HA microspheres (**Fig. 3b**). However, it was still only approximately half the value for a reference β-TCP material with the same surface area.

Degradation of the hollow HA and CHA microspheres by osteoclast-like cells was also observed in vitro, indicating that the microspheres were susceptible to both solution-mediated and cell-mediated resorption. Previous studies showed that osteoclastic degradation of HA was dependent on its composition, crystallinity and grain size [27–30]. Carbonate-substituted HAs with an amorphous structure or a fine grain size were found to be more susceptible to degradation. In the present study, the hollow CHA microspheres with

12 wt. % carbonate appeared to show more extensive degradation than the HA microspheres by osteoclast-like cells but the amount of degradation could not be readily quantitated. There was no observable difference in osteoclast adhesion to the surface of the HA and CHA microspheres. While surface roughness and grain size can influence cell adhesion [48, 49], the osteoclasts (~50 μm) were much larger than differences in the surface roughness, grain size and pore size of the microspheres (less than a few tens of nanometers).

However, in this in vitro study, no significant difference of osteoclast adhesion and osteoclastic differentiation was observed between the HA and CHA groups. It was reported the implant surface roughness and grain size could affect cell adhesion [48, 49], but the osteoclasts are much larger in size comparing to the differences of roughness, grain size and pore size between the two types of microspheres.

4.2 Resorption of hollow microspheres and bone regeneration in vivo

Resorption of the hollow HA and CHA12 microspheres without BMP2 in rat calvarial defects was evaluated at 12 weeks postimplantation from the number of open microspheres as a percentage of the total number of microspheres in the defect site. Degradation of the microspheres was clearly visible in the form of open microspheres in which a segment of the shell was missing (**Fig. 5a, b**). The percent open microspheres in the defect implanted with the CHA12 microspheres was significantly greater than the HA group. Solution-mediated resorption of the hollow microspheres is expected to be approximately homogeneous, leading to a gradual reduction in the shell thickness. In comparison, osteoclastic resorption is expected to be more rapid, resulting in more rapid degradation of the portions of the shell where the osteoclasts were attached. The combination of solution-mediated and cell-mediated resorption presumably resulted in the formation of the open microspheres within the twelve-week implantation period.

Bone regeneration in the defects implanted with the HA or CHA12 microspheres (without BMP2) was limited, as observed in our previous study for HA microspheres implanted in the same osseous defect model [33]. Loading the HA and CHA12 microspheres with BMP2 (1 μg per defect) significantly enhanced the capacity of both groups to regenerate bone in the defects. The enhancement of bone regeneration in the defects implanted with the BMP2-loaded HA microspheres is consistent with the results of our previous study [33].

It was also found that the BMP2-loaded CHA12 microspheres had a faster resorption rate than the HA microspheres with BMP2 and the CHA12 microspheres without BMP2. The amount of residual BMP2-loaded CHA12 microspheres in the defects at 12 weeks postimplantation (7 ± 2%) was significantly lower than the BMP2-loaded HA microspheres (21 ± 3%) and the CHA12 microspheres without BMP2 (28 ± 8%). The faster resorption of the BMP2-loaded CHA12 microspheres (when compared to the CHA12 microspheres without BMP2) could be explained in terms of the dual function of BMP2 in controlling bone formation and bone resorption [50]. Briefly, the Smad pathways activated by BMPs play a central role in BMP signaling by activating osteoblastogenesis [51]. However, the Smad pathways activated by BMPs also activate the bone resorption process which involves the expression of BMP antagonists such as Noggin and Sclerostin (SOST), both of which are also secreted from osteoblasts [52]. SOST eventually enhances resorption by triggering

receptor activator of nuclear factor-kappa B ligand (RANKL)-osteoprotegerin pathway-induced osteoclastogenesis [53]. In the present study, the enhancement of osteoclastic differentiation by BMP2 can lead to faster degradation of the BMP2-loaded CHA12 microspheres in the rat calvarial defects when compared to the CHA12 microspheres without BMP2.

The percent new bone in the defects implanted with the BMP2-loaded CHA12 microspheres (73 ± 9%) was significantly greater than the BMP2-loaded HA microspheres (59 ± 2%). Because of the faster degradation of the CHA12 microspheres, a larger amount of pore space was available for new bone infiltration, resulting in a significantly larger amount of new bone in the defects implanted with the CHA12 microspheres.

The BMP2 dose used in the present study (1 μg per defect) was identical to the dose used in our previous study [33] and within the range of doses used in previous studies for the rat calvarial defect model [54–56]. It is also well below the dose found to cause adverse biological effects in the same animal model [57]. However, the optimal BMP2 dose for the CHA microspheres and the animal model used in the present study was not investigated. Furthermore, the amount of carbonate in the CHA12 microspheres evaluated in vivo (12.4 wt. %) was higher than the value (~8 wt. %) in human bone. A range of BMP2 doses and CHA microspheres with different carbonate content should be investigated in future studies. In general, the results of the present study indicate that the combination of carbonate-substituted hydroxyapatite microspheres and a clinically safe dose of BMP2 could provide a promising system to stimulate bone regeneration and enhance implant resorption in healing non-loaded bone defects.

5. Conclusions

Hollow hydroxyapatite (HA) microspheres, with a high-surface-area mesoporous shell, were prepared with controllable amounts of carbonate substitution (0–12 wt. %) using a novel glass conversion route at 37 °C. Hollow HA microspheres with 12.4 wt. % of carbonate (designated CHA12) showed a higher surface area (236 m^2g^{-1}) than hollow HA microspheres prepared conventionally (179 m^2g^{-1}) and a faster degradation rate in a potassium acetate buffer solution in vitro. When implanted for 12 weeks in rat calvarial defects, the CHA12 and HA microspheres showed a limited capacity to regenerate bone but the CHA12 microspheres resorbed faster than the HA microspheres. Loading the microspheres with bone morphogenetic protein-2 (BMP2) (1 μg per defect) stimulated bone regeneration and accelerated the resorption of the CHA12 microspheres in the defects. The amount of new bone in the defects implanted with the BMP2-loaded CHA12 microspheres was significantly greater than the HA microspheres while the amount of residual CHA12 microspheres was significantly lower than the HA microspheres. The combination of these carbonate-substituted HA microspheres with clinically safe doses of BMP2 could provide promising implants for healing non-loaded bone defects.

Acknowledgement

Supported by the National Institutes of Health, National Institute of Dental and Craniofacial Research, Grant Number 1R15DE023987-01.

References

1. Laurencin C, Khan Y, EI-Amin SF. Expert Rev Med Devices. 2006; 3:49–57. [PubMed: 16359252]
2. Giannoudis PV, Dinopoulos H, Tsiridis E. Injury. 2005; 36(Suppl 3):S20–7. [PubMed: 16188545]
3. Neovius E, Engstrand T. J Plast Reconstr AES. 2010; 63:1615–23.
4. Dahlin C, Johansson A. Clin Implant Dent R. 2011; 13:305–10.
5. Stahl SS, Froum SJ. J Periodontol. 1987; 58:689–95. [PubMed: 2822889]
6. Turunen T, Peltola J, Yli-Urpo A, Happonen RP. Clin Oral Implants Res. 2004; 15:135–41. [PubMed: 15008925]
7. Rickert D, Slater JJ, Meijer HJ, Vissink A, Raghoebar GM. Int J Oral Maxillofac Surg. 2012; 41:160–7. [PubMed: 22099314]
8. Tadjoedin ES, de Lange GL, Lyaruu DM, Kuiper L, Burger EH. Clin Oral Implants Res. 2002; 13:428–36. [PubMed: 12175381]
9. Wikesjo UM, Qahash M, Huang YH, Xiropaidis A, Polimeni G, Susin C. Orthod Craniofac Res. 2009; 12:263–70. [PubMed: 19627529]
10. Polo CI, Oliveira Lima JL, De Lucca L, Piacezzi CB, Naclerio-Homem MG, Arana-Chavez VE, Sendyk WR. J Periodontol. 2013; 84:360–70. [PubMed: 22524330]
11. Reichert JC, Cipitria A, Epari DR, Saifzadeh S, Krishnakanth P, Berner A, Woodruff MA, Schell H, Mehta M, Schuetz MA, Duda GN, Hutmacher DW. Sci Transl Med. 2012; 4:141ra93.
12. Bohner M. Injury. 2000; 31:D37–47.
13. Dorozhkin SV. BIO. 2011; 1:1–51.
14. LeGeros R. Z. Clin Orthop Rel Res. 2002; 395:81–98.
15. Bose S, Tarafder S. Acta Biomater. 2012; 8:1401–21. [PubMed: 22127225]
16. Alam MI, Asahina I, Ohmamiuda K, Enomoto S. J Biomed Mater Res. 2001; 54:129–38. [PubMed: 11077412]
17. Yuan H, De Bruijn JD, Zhang X, Van Blitterswijk CA, de Groot K. J Mater Sci Mater Med. 2001; 12:761–6. [PubMed: 15348221]
18. Ruhé P, Kroese-Deutman H, Wolke J, Spauwen P, Jansen J. Biomaterials. 2004; 25:2123–32. [PubMed: 14741627]
19. Gonda Y, Shibata Y, Okuda T, Kawachi G, Kamitakahara M, Murayama H, et al. Biomaterials. 2009; 30:4390–4400. [PubMed: 19481798]
20. Tazaki J, Murata M, Akazawa T, Yamamoto M, Ito K, Arisue M, Shibata T, Tabata Y. Biomed Mater Eng. 2009; 19:141–6. [PubMed: 19581707]
21. Notodihardjo FZ, Kakudo N, Kushida S, Suzuki K, Kusumoto K. J Cranio Maxill Surg. 2012; 40:287–91.
22. LeGeros, RZ. Monogr Oral Sci. Vol. 15. Karger; Basel: 1991. p. 4-45.
23. LeGeros RZ. Clin Mater. 1993; 14:65–88. [PubMed: 10171998]
24. Klein CPAT, Patka P, den Hollander W. Biomaterials. 1989; 10:59–62. [PubMed: 2540845]
25. Doi Y, Iwanaga H, Shibutani T, Moriwaki Y, Iwayama Y. J Biomed Mater Res. 1999; 47:424–33. [PubMed: 10487896]
26. Leeuwenburgh S, Layrolle P, Barrère F, de Bruijn J, Schoonman J, van Blitterswijk CA, de Groot K. J Biomed Mater Res. 2001; 56:208–15. [PubMed: 11340590]
27. Doi Y, Shiutani T, Moriwaki Y, Kajimoto T, Iwayama Y. J Biomed Mater Res. 1998; 39:603–10. [PubMed: 9492222]
28. Klein CPAT, Driessen AA, De Groot K, van den Hooff A. J Biomed Mater Res. 1983; 17:769–84. [PubMed: 6311838]
29. LeGeros RZ, Parsons JR, Daculsi G, Driessens F, Lee D, Liu ST, Metsger S, Perterson D, Walker M. Ann New York Acad Sci. 1988; 523:268–71. [PubMed: 2837944]
30. Baig AA, Fox JL, Su J, Wang Z, Otsuka M, Higuchi WI, Legeros RZ. J Colloid Interface Sci. 1996; 179:608–17.
31. Fu H, Rahaman MN, Day DE, Fu Q. J Am Ceram Soc. 2010; 93:3116–23. [PubMed: 21892226]

32. Fu H, Rahaman MN, Day DE, Brown RF. J Mater Sci Mater Med. 2011; 22:579–91. [PubMed: 21290170]
33. Xiao W, Fu H, Rahaman MN, Liu Y, Bal BS. Acta Biomater. 2013; 9:8374–83. [PubMed: 23747325]
34. Jarco M. Clin Orthop. 1981; 157:259–78. [PubMed: 7018783]
35. Roy M, Bose S. J Biomed Mater Res A. 2012; 100:2450–61. [PubMed: 22566212]
36. Lin Y, Xiao W, Liu X, Bal BS, Bonewald LF, Rahaman MN. J Non-Cryst Solids. 2015 DOI: 10.1016/j.jnoncrysol. 2015.04.008.
37. Clark AE, Hench LL. J Non-Cryst Solids. 1989; 113:195–202.
38. Filgueiras MR, LaTorre G, Hench LL. J Biomed Mater Res. 1993; 27:445–53. [PubMed: 8385143]
39. Patel N, Best SM, Bonfield W. J Aust Ceram Soc. 2005; 41:1–22.
40. LeGeros RZ, LeGeros JP, Trautz RO, Klein E. Dev Appl Spectrosc. 1970; 7B:12–22.
41. Hayashi C, Hasegawa U, Saita Y, Hemmi H, Hayata T, Nakashima K, Ezura Y, Amagasa T, Akiyoshi K, Noda M. J Cell Physiol. 2009; 220:1–7. [PubMed: 19301257]
42. Hong SJ, Kim CS, Han DK, Cho IH, Jung UW, Choi SH, Kim CW, Cho KS. Biomaterials. 2006; 27:3810–6. [PubMed: 16574220]
43. Chung YI, Ahn KM, Jeon SH, Lee SY, Lee JH, Tae G. J Control Release. 2007; 121:91–9. [PubMed: 17604871]
44. Driessens, FCM. Bioceramics of Calcium Phosphate. De-Groot, K., editor. CRC Press; Boca Raton, FL: 1983. p. 1-32.
45. LeGeros RZ, Miravite MA, Quirolgico GB, Curzon MEJ. Nature. 1965; 205:403–4. [PubMed: 14243434]
46. LeGeros RZ, Trautz OR, LeGeros JP, Klein E. Science. 1967; 155:1409–11. [PubMed: 17839613]
47. Pan H, Darvell BW. Cryst Growth Des. 2000; 10:845–50.
48. Schwartz Z, Lohmann CH, Oefinger J, Bonewald LF, Dean DD, Boyan BD. Adv Dent Res. 1999; 13:38–48. [PubMed: 11276745]
49. Boyan BD, Bonewald LF, Paschalis EP, Lohmann CH, Rosser J, Cochran DL, Dean DD, Schwartz Z, Boskey AL. Calcif Tissue Int. 2002; 71:519–29. [PubMed: 12232675]
50. Kim RY, Oh JH, Lee BS, Seo YK, Hwang SJ, Kim IS. Biomaterials. 2014; 35:1869–81. [PubMed: 24321706]
51. Noth U, Tuli R, Seghatoleslami R, Howard M, Shah A, Hall DJ, Hickok NJ, Tuan RS. Exp Cell Res. 2003; 291:201–11. [PubMed: 14597420]
52. Kamiya N, Kobayashi T, Mochida Y, Yu PB, Yamauchi M, Kronenberg HM, Mishina Y. J Bone Miner Res. 2010; 25:200–10. [PubMed: 19874086]
53. Kamiya N, Ye L, Kobayashi T, Mochida Y, Yamauchi M, Kronenberg HM, Feng JQ, Mishina Y. Development. 2008; 135:3801–11. [PubMed: 18927151]
54. Zhao J, Shen G, Liu C, Wang S, Zhang W, Zhang X, Zhang YD, Wei J, Zhang Z, Jiang X. Tissue Eng A. 2012; 18:185–97.
55. Lee JH, Kim CS, Choi KH, Jung UW, Yun JH, Choi SH, Cho KS. Biomaterials. 2010; 31:3512–9. [PubMed: 20149447]
56. Marden LJ, Hollinger JO, Chaudhari A, Turek T, Schaub RG, Ron E. J Biomed Mater Res A. 1994; 28:1127–38.
57. Cowan CM, Aghaloo T, Chou YF, Walder B, Zhang X, Soo C, Ting K, Wu B. Tissue Eng. 2007; 13:501–12. [PubMed: 17319794]

Highlights

- Creation of high-surface-area hollow hydroxyapatite microspheres with controlled amounts of carbonate substitution using a novel glass conversion route near room temperature
- The carbonate-substituted hydroxyapatite (CHA) microspheres are biodegradable, unlike most synthetic HA that are almost bioinert
- When loaded with BMP2, the CHA microspheres degrade almost completely and heal defects in rat calvaria within 12 weeks
- These CHA microspheres loaded with safe doses of BMP2 are promising for healing defects in non-loaded bone

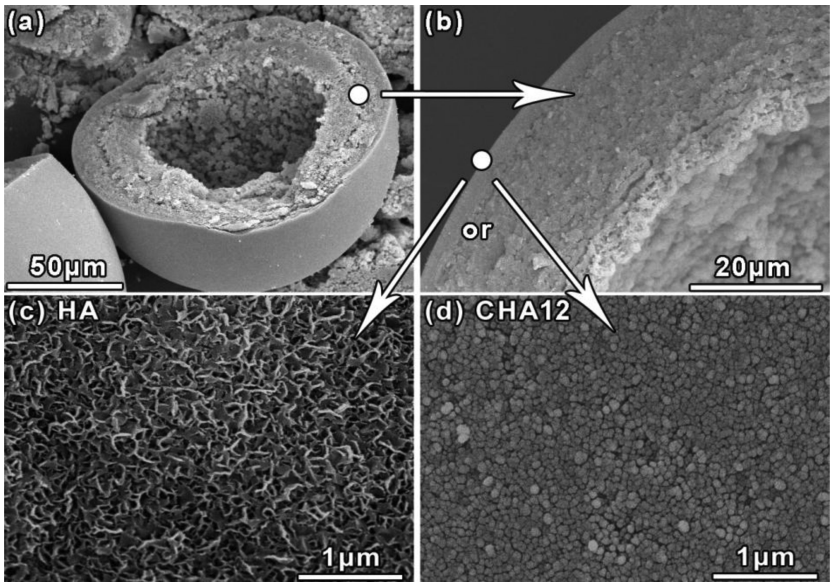

Fig. 1.

SEM images of the cross section of a hollow HA microsphere (a, b) and higher magnification images showing differences in surface morphology between the hollow HA and CHA12 microspheres (c, d).

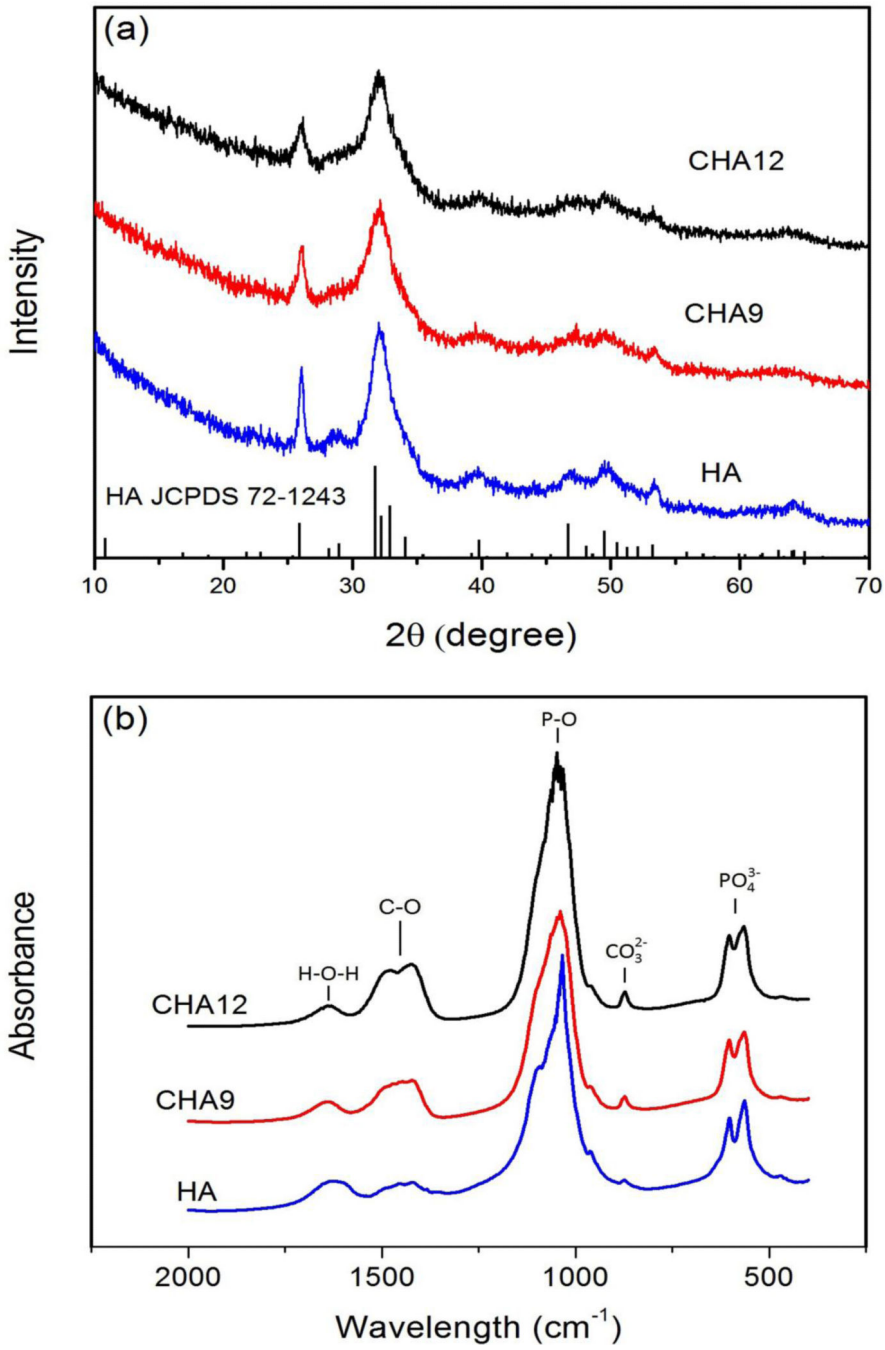

Fig. 2.

(a) X-ray diffraction patterns and (b) FTIR spectra of the hollow HA, CHA9 and CHA12 microspheres. The pattern of a reference hydroxyapatite (HA JCPDS 72-1243) is also shown in (a).

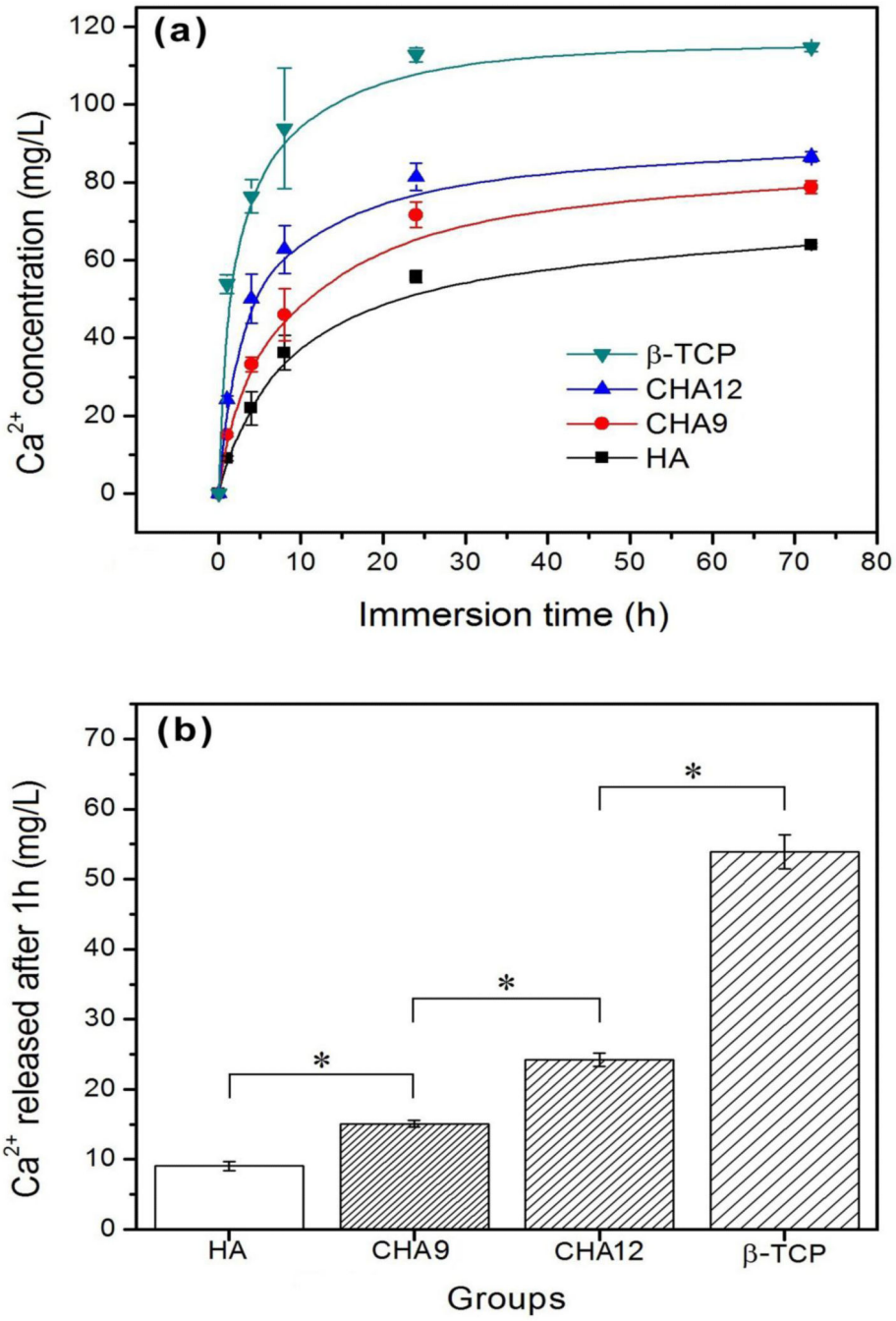

Fig. 3.

(a) Cumulative amount of Ca^{2+} ion released from hollow HA, CHA9, and CHA12 microspheres into 0.1 M potassium acetate buffer solution (pH = 5.0; 37 °C) as a function of immersion time. (b) Amount of Ca^{2+} ions released from the three groups of microspheres after 1 h in the buffer solution. For comparison, the release of Ca^{2+} ions from a β-TCP reference material is also shown. (*significant difference between groups; $p<0.05$)

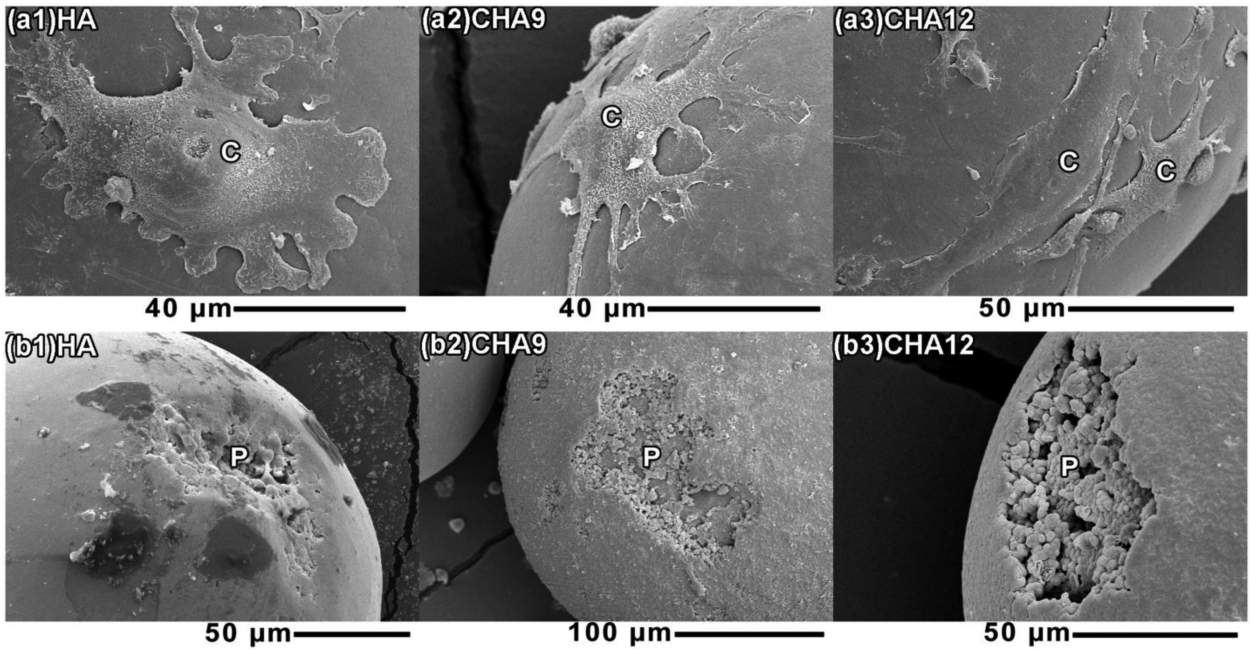

Fig. 4.

SEM images of the surface of the HA, CHA9 and CHA12 microspheres after incubation with TIB-71 cells with added RANKL for 1 week (a1-3), and after the cells had been rinsed off (b1-3). (C: cells; P: pitted area after removal of cells)

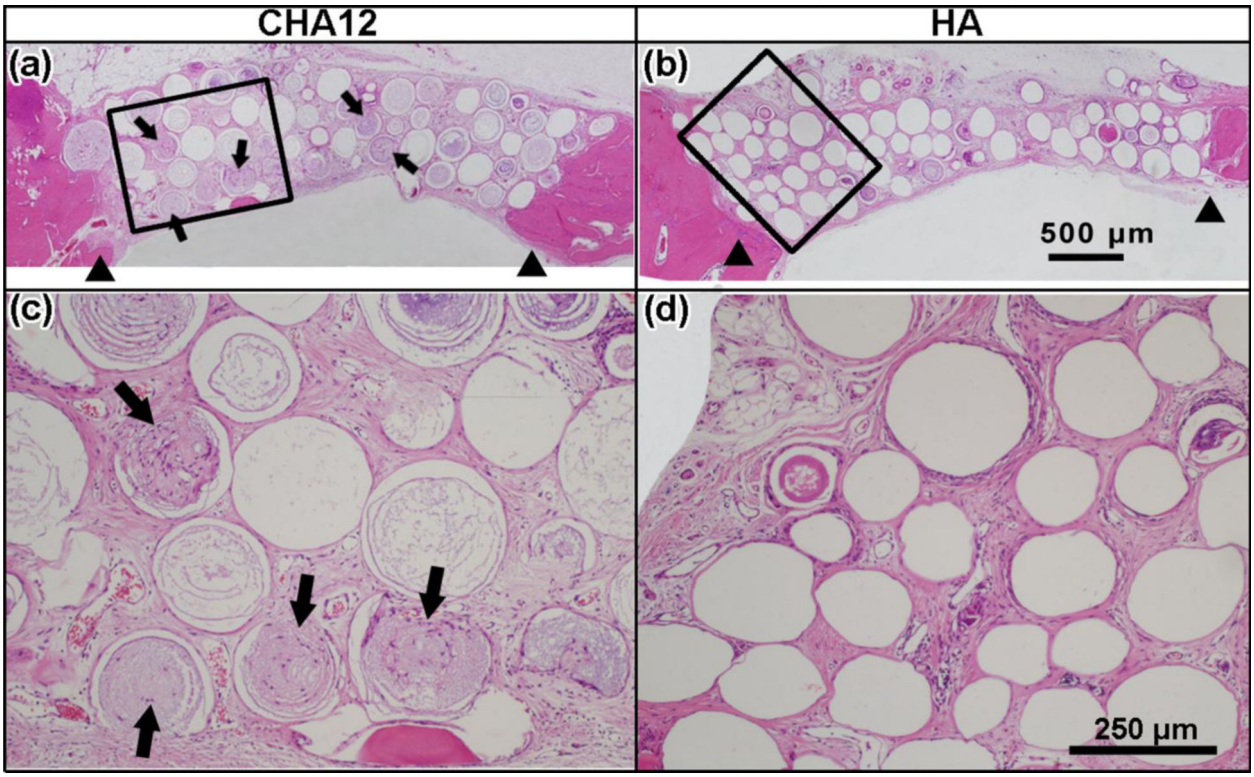

Fig. 5.

Transmitted light images of (a, b) H&E stained sections of rat calvarial defects implanted with hollow CHA12 and HA microspheres without BMP2 at 12 weeks postimplantation; (c, d) higher magnification images of the boxed areas in a, b. (Arrowheads: edges of host bone; arrows: open microspheres)

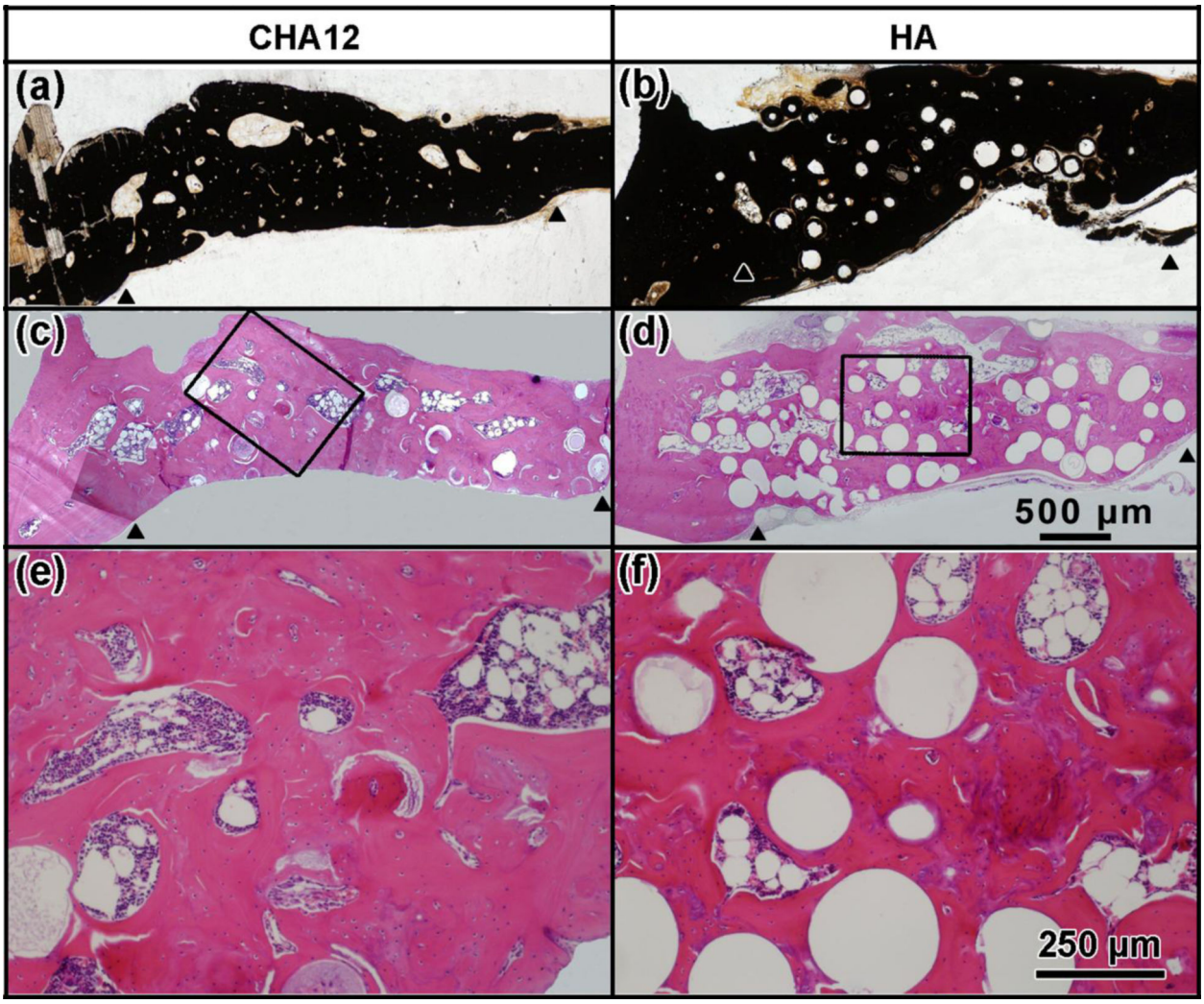

Fig. 6.

Transmitted light images of (a, b) von Kossa and (c, d) H&E stained sections of rat calvarial defects implanted with hollow CHA12 and HA microspheres loaded with BMP2 at 12 weeks postimplantation; (e, f) higher magnification images of the boxed areas in c, d. (Arrowheads: edges of host bone)

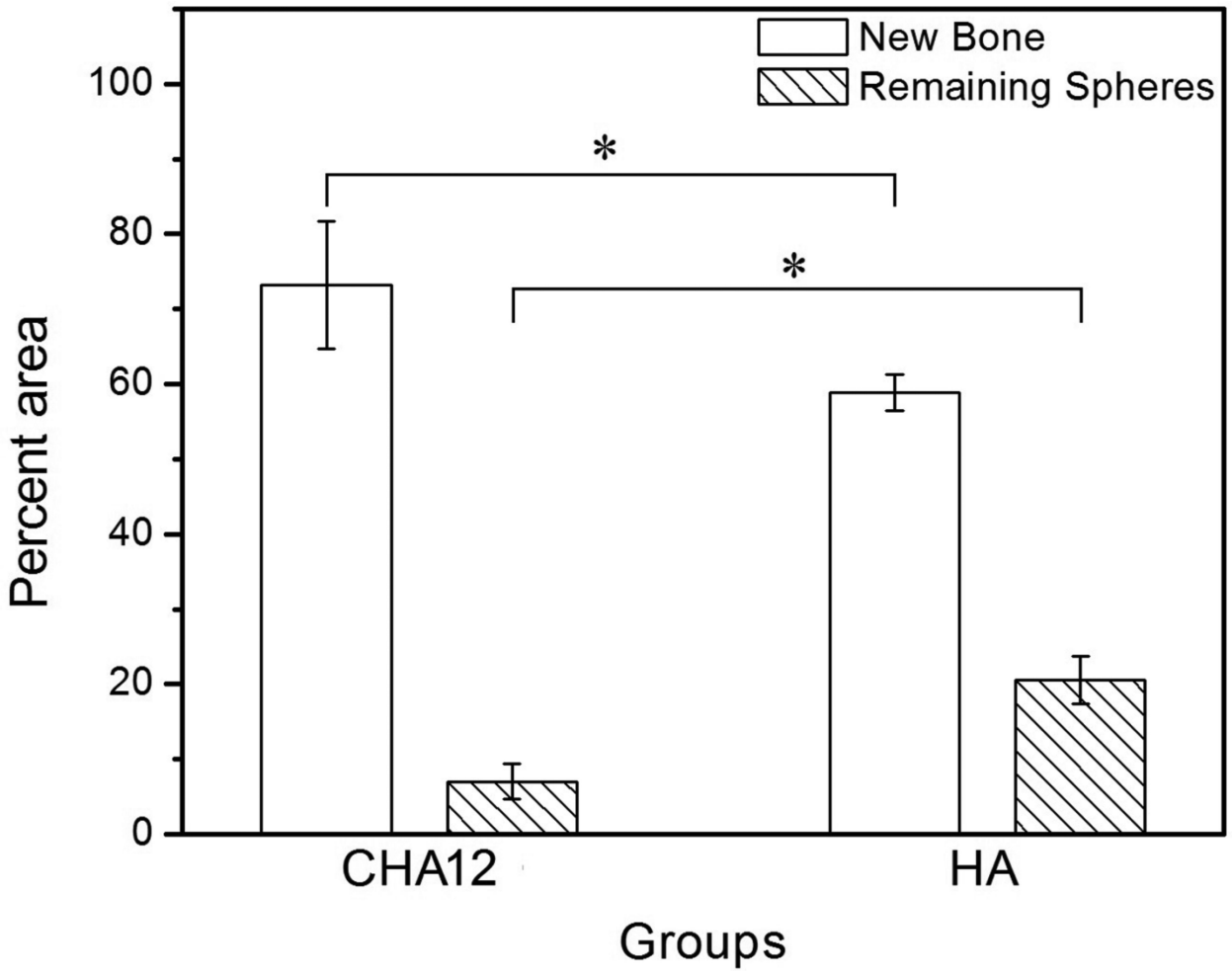

Fig. 7.

New bone and residual amount of microspheres, as a percentage of the total defect area, in rat calvarial defects implanted with CHA12 and HA microspheres loaded with BMP2 at 12 weeks postimplantation. (*significant difference between groups; $p<0.05$)

Table I

Characteristics of hollow hydroxyapatite (HA) and carbonate-substituted hydroxyapatite (CHA) microspheres prepared by converting borate glass microspheres (150–250 μm) in 0.02 M K_2HPO_4 solution containing different concentrations of $KHCO_3$ at 37 °C. Data for commercial β-TCP granules used as the control group are included for reference.

Microsphere designation	$KHCO_3$ concentration (M) in solution	CO_3 content of microspheres (wt. %)	Surface area of microspheres (m^2g^{-1})	Average pore size of shell (nm)	Microsphere diameter (μm)
HA	0	2.1*	179	11	150–250
CHA9	0.135	8.6	233	8	150–250
CHA12	0.27	12.4	236	7	150–250
β-TCP			0.30		53–124#

*Presumably due to dissolved CO_2 in the aqueous medium

#granule size